International Journal of Engineering Trends and Technology
ISSN: 2231-5381/ https://doi.org/10.14445/22315381/IJETT-V74I8P101
Volume 74 Issue 8, 1-18, August 2026

Original Article

Thermal Degradation and Residual Strength Assessment of Reinforced Concrete Members Exposed to Elevated Temperatures

Bilal Siddiqui[1], Neha Mumtaz[1*], Tabish Izhar[1], Syed Aqeel Ahmad[1]

[1]*Department of Civil Engineering, Integral University, Lucknow, U.P., India.*

[*]*Corresponding Author : nehamumtaz@iul.ac.in*

Received: 16 April 2026 Revised: 21 May 2026 Accepted: 03 June 2026 Published: 29 August 2026

Abstract - *This research involves the degradation of RC members upon exposure to fire and studying their residual strength behavior. The temperature was elevated upto 1050°C with focus on its cooling regimes using air cooling and water quenching. Experimental evaluation was conducted using compressive strength, flexural strength, and Ultrasonic Pulse Velocity (UPV) measurements. This was accompanied by microstructural analysis through Scanning Electron Microscopy (SEM-EDS). The results indicate that concrete retains most of its mechanical integrity up to 200-250°C, followed by progressive degradation beyond 400°C, with critical strength loss occurring in the range of 600-800°C. Water-cooled specimens exhibited relatively improved residual performance at higher temperatures. At the same time, air-cooled specimens showed greater deterioration due to prolonged thermal exposure. UPV measurements demonstrated a strong correlation with internal damage and residual strength. This confirms their effectiveness as a non-destructive evaluation technique. Microstructural observations revealed increased porosity, Interfacial Transition Zone (ITZ) cracking, and decomposition of hydration products at elevated temperatures, which directly contributed to strength reduction. Using the experimental data, a regression-based predictive model was developed to correlate residual compressive strength with temperature and UPV. The model demonstrated strong agreement with experimental results, achieving a prediction accuracy exceeding 90%. The findings provide a comprehensive understanding of the thermo-mechanical behavior of RC members under fire exposure. Overall, it highlights the potential of combining non-destructive testing with predictive modeling for reliable post-fire structural assessment.*

Keywords - *Elevated temperature, Fire damage, Residual strength, Cooling method, Ultrasonic Pulse Velocity, Reinforced concrete.*

1. Introduction

Concrete is a mix of a cement-based binding agent (usually Portland cement), small and large stones (aggregates), and water that turns solid through a process called hydration. Concrete is great at resisting being crushed, but not so good at being stretched, so steel is added to RC to handle the stretching forces and make it more flexible [1, 2]. Fire's intense heat changes concrete in both its physical form and its chemistry; the paste holding it together loses its water. The water inside becomes steam, and the heat creates stresses that split the concrete with cracks, which leads to a weaker structure.

Reinforced concrete buildings are usually fairly good at withstanding fire and are designed to remain safe for as long as a fire is expected to last (according to the rules for buildings) because concrete is a slow conductor of heat, sheltering the steel inside. However, if a fire reaches critical temperatures and goes on for a long time, the materials deteriorate considerably. So, after the fire, it needs to determine how much strength is left to decide whether to fix or completely rebuild [3].

Extensive research indicates a direct correlation between increased concrete temperature and reduced compressive strength. This loss of strength happens progressively and is considerable: typical concrete will lose about half of its crushing strength around 600°C and almost all of it above 800°C [4-6]. For instance, heating to 200°C, 400°C, 600°C, and 1000°C reduces compressive strength by roughly 18%, 37%, 42% and 73% compared to the strength at room temperature. Around 400-500°C, a point is often reached where strength starts to fall off quickly as the key parts of the hydrated cement break down. Above this, the strength loss speeds up, and at 800°C, typical concrete of normal strength might have only 80% or less of its original strength [7, 8]. This deterioration happens because of several changes at a microscopic level: the different ways the aggregate and cement paste expand with heat create internal stress and small cracks, water is lost from things like calcium hydroxide and Calcium-Silicate-Hydrate (C-S-H) which are the binding components of the cement paste, and as water escapes, pores become larger, steam builds up in any sealed pores at high temperatures and can cause the concrete to explode (spall), and when it cools, rehydration of lime and thermal contraction can create more cracks [9-11]. Examining the concrete with a Scanning Electron Microscope (SEM) confirms that after a fire, it has larger pores, tiny cracks, and a breakdown of the material holding it together - and these changes in the material's structure match the drop in compressive and flexural strength.

Researchers also observed that when concrete is heated to extreme temperatures, significant residual damage is unavoidable, making post-fire assessment techniques critical [12, 13]. Non-destructive evaluation methods such as Ultrasonic Pulse Velocity (UPV) measurements are widely used to assess internal damage in heated concrete. As concrete deteriorates, UPV decreases (and transit time of the pulse increases) due to the development of cracks and loss of solid continuity. By comparing pulse travel times or velocities before and after fire, one can infer the severity of internal cracking and strength loss. Many post-fire evaluation protocols combine visual inspection, UPV, and core strength tests to quantify damage [14, 15].

After high-temperature exposure, an important parameter in the post-fire condition of concrete is the proposed cooling method. Cooling has a pronounced effect on residual properties. Letting the concrete cool slowly (air) allows the stresses from the heat to ease off gradually. Conversely, rapidly cooling it (water) causes 'thermal shock'. Other research has found that concrete that's suddenly cooled with water can lose an extra 30-40% of its strength, compared to concrete cooled naturally, at the same highest temperature. For instance, Bingöl and Gül observed that after heating to 400 °C, air-cooled concrete retained 80% of its original strength, whereas water-quenched concrete retained only 70% (i.e. 30% strength loss vs 20% for air-cooled) [16-19]. This negative effect of water cooling is most obvious at moderately high temperatures (roughly 200-500°C) because at these temperatures, the temperature difference within the concrete is enough to create cracking, but the concrete has not yet lost all of the water within it. The cooling regime influences the residual pore structure - water quenching tends to increase residual porosity and crack network, leading to lower strength. Kim et al. similarly concluded that a faster cooling rate exacerbates aggregate-paste interface thermal mismatch and produces greater dimensional distortion and micro-cracking. However, at high temperatures (close to 1000 °C), the difference between cooling methods becomes less significant, as the concrete is already extensively cracked and degraded by heat. In these situations, both air-cooled and water-cooled concrete will have very little strength left (often less than force of the original 20-30%). Some research even suggests water cooling might be slightly beneficial at extremely high temperatures, as quickly cooling it down can prevent the concrete from being at a high temperature for a long time and could put some of the water back into the dehydrated cement parts, helping them stick together again. Generally, though, the research indicates that air cooling will leave more strength than water cooling if the concrete has not been heated too much, but if it has been very hot (800°C or more), it is in bad shape, however it is cooled, and water cooling can sometimes leave a little more strength for pushing or bending [20, 21].

Previous existing studies on fire-exposed concrete mainly focus on strength degradation or isolated material behavior. Furthermore, the combined influence of cooling regimes, non-destructive evaluation techniques such as Ultrasonic Pulse Velocity (UPV), and microstructural characterization has not been comprehensively addressed.

This study addresses these gaps by combining experimental, microstructural, and predictive approaches (compressive and flexural strength, correlation with UPV measurements, and microstructural assessment using SEM-EDS). To estimate the residual strength based on thermal exposure and cooling conditions, a predictive framework is proposed.

2. Materials and Methodology

2.1. Materials and Specimen Preparation

The experimental program included 150 mm concrete cubes and RC beams of size 150 × 150 × 700 mm. Specimens were exposed to temperatures ranging from 200°C to 1050°C. Air cooling and water quenching were adopted for each condition. The tests conducted included compressive strength, flexural strength, Ultrasonic Pulse Velocity (UPV), and SEM-EDS analysis. Ordinary Portland Cement (OPC) was used as the binder for all mixes, with the properties shown in Table 1. A single concrete mix design was used for all specimens to ensure comparability. The mix was proportioned for a target 28-day compressive strength of about 30 MPa.

Table 1. Materials and specimen properties

S.No.	Parameters	
1.	Standard Consistency	Value
2.	Initial Setting Time	34%
3.	Final Setting Time	37 Minutes
4.	Fineness	575 Minutes
5.	Specific Gravity	4.39
6.	Compressive strength (3 days)	3.16
7.	Compressive strength (7 days)	4.76 MPa

The freshly mixed concrete slumped 75mm, which is appropriate to flow nicely into moulds without the ingredients separating. The standard procedures for pouring are adopted: a rotating mixer for mixing, the cubes poured into steel moulds and vibrated to remove air bubbles, and the beams filled in layers with plenty of prodding and shaking, then vibrated on the outside to eliminate any trapped air.

After 28 days of curing (room temperature), allowing the cement to set fully and the concrete to gain almost all of its strength before any heat was applied. Before the heating began, each sample's initial characteristics were noted: its weight (to the nearest gram), dimensions (calipers and a steel tape measure were used for the beams' length), and the speed of sound travelling through it (ultrasonic pulse velocity).

The test was done by measuring the initial speed of sound by putting sensors on opposing faces (for cubes) or ends (for beams) and timing how long it took a 54 kHz sound pulse to pass through the concrete. The three cubes from the control group were tested (not heated), and they averaged 32.5 MPa, showing the mix was as strong as planned.

Similarly, three control beams were tested in flexure under four-point bending (per IS 516 or ASTM C78) to determine the modulus of rupture at ambient conditions, which averaged 6.9 MPa. These control values serve as references to evaluate residual strength after high-temperature exposure.

2.2. High-Temperature Exposure Protocol

After curing, specimens were subjected to elevated temperatures in an electric Diesel furnace with internal dimensions sufficient to accommodate either three cubes or one beam per heating run (the beams were heated individually due to their size). To ensure uniform heating, specimens were placed such that all faces were exposed (for cubes) or all sides of the beam were heated (the beam was on supports in the furnace, allowing roughly uniform heating around its perimeter) as shown in Figure 1. The furnace temperature was controlled via a programmable logic controller to follow the desired heating profile.

Fig. 1 Placement of casted cubes and beams in diesel furnace

Target peak temperatures were selected as 200 °C, 400 °C, 600 °C, 800 °C, and 1000 °C, representing a range from mild to extreme thermal exposure as shown in Figure 2. In each test, the furnace was ramped at approximately 5-10 °C per minute up to the target temperature. When the intended temperature was achieved, it was kept steady for 2 hours. This allowed the concrete in the middle to get close to the same temperature as the furnace and mimic a long-lasting fire.

After this period of being held at a temperature, the furnace was turned off, and the samples were left to cool in one of two ways: natural air cooling. With natural air cooling, the furnace door was opened, and the sample was allowed to cool in still air inside the furnace room. Cooling was fairly gradual; the surface went from 1000°C to around 100 °C in 2 hours, and to room temperature in a full 24 hours.

Fig. 2 Specimen exposed to fire in an electric diesel furnace

2.3. Water Quenching (WQ)

The hot specimen was immediately removed from the furnace at peak temperature using tongs and immersed in a large tank of water at 20 °C. This sudden quenching caused vigorous boiling at the concrete surface. Specimens were kept submerged for about 30 minutes until fully cooled. This simulates firefighting actions where cold water is sprayed on hot concrete, causing a severe thermal shock. It is acknowledged that the number of beam replicates was limited (1-2 per condition) due to furnace size constraints, which is a limitation of the present study. Each temperature range had at least three specimens per cooling method for statistical reliability.

No explosive spalling was observed in our tests, likely because the concrete was air-dried for a few days before heating (reducing internal moisture) and had no dense siliceous aggregate that might undergo sudden phase changes.

Minor surface cracking and color changes were noted: specimens turned reddish-pink around 300 °C (due to hematite formation from iron compounds) and gray/whitish at 600-800 °C (due to dehydration of cement paste), as shown in Figure 3. By 1000 °C, cube corners had rounded slightly, and surfaces showed micro-cracks, but overall geometry remained intact.

Fig. 3 Specimen after fire exposure at different temperatures (visible cracks)

2.4. Post-Fire Testing Procedures

After cooling (either by air or water), the specimens were tested to determine their residual properties. To figure out how much mass was lost due to the heat, each sample was weighed on the same scale as its original weighing. The percentage of mass lost is calculated.

This demonstrates how the concrete as a whole got bigger or smaller with the heat, and whether it bent or twisted permanently.

Because concrete does not expand much at moderate temperatures and tends to shrink as it cools from high temperatures, no big change was shown.

2.5. Ultrasonic Pulse Velocity (UPV) Testing

Once cooled, the samples were again tested for sound speed to identify any damage inside (as shown in Figure 4). For the cubes, the sound pulse travelled directly from one face to the other (150mm apart), and the time it took to do so was recorded.

For beams, UPV was measured in two orientations: (1) across the cross-section (150 mm path length, transmitter and receiver on opposite faces of the beam's mid-span cross-section) to gauge local damage in the concrete cover, and (2) along the length (transmitter at one end of the beam, receiver at the other end, 700 mm path) to see if a pulse could travel through the entire span.

Fig. 4 Ultrasonic Pulse Velocity (UPV) testing of specimen

The latter essentially checks for severe cracking or discontinuities along the beam. At higher temperatures, the long-path signal was often too attenuated to be received. The pulse velocity was calculated (path length divided by transit time) for cases where a clear signal was obtained. UPV is sensitive to internal micro-cracking: a significant increase in transit time (or drop in velocity) after fire indicates stiffness degradation and cracking inside the concrete. The transit times were recorded to the nearest 0.1 µs; for cases with no detectable through-signal (e.g. 700 mm path at 800-1000 °C), the transit time was recorded as "no signal" (effectively infinite time).

2.6. Destructive Strength Testing

Finally, the mechanical strengths of the cooled specimens were measured. Cube compressive strength was tested in a 3000 kN capacity hydraulic testing machine as per IS:516, as shown in Figure 5. Each cube was loaded to failure, and the maximum load was recorded. Residual compressive strength was computed (load divided by original cross-sectional area, 225 cm²).

Flexural testing of beams was conducted under a four-point bending setup (two-point loads at third-span locations). The load was applied by a hydraulic jack and measured with a load cell; deflection at mid-span was monitored to identify the yield and ultimate points.

The beams, having a reinforcement ratio of 1%, were under-reinforced, so failure was by concrete crushing at higher temperatures (since the steel had largely yielded or lost strength).

The peak load was used to back-calculate an equivalent flexural tensile stress (modulus of rupture) using the formula. $f_r = \frac{M}{S}$, where M is the maximum moment and S the section modulus of the beam cross-section. For simplicity, the 'equivalent flexural stress' is definedas-

$$f = \frac{P_{max}L}{4bd^2}$$

(for a beam of span L, breadth $b = 150$ mm, depth $d = 150$ mm under four-point loading). Although the beams contained steel, at high temperatures, the steel's yield strength is reduced; after cooling, the steel can regain strength, but bond damage and concrete cracking often govern the beam capacity. The measured flexural stress serves as an index for the beam's residual load-bearing capacity.

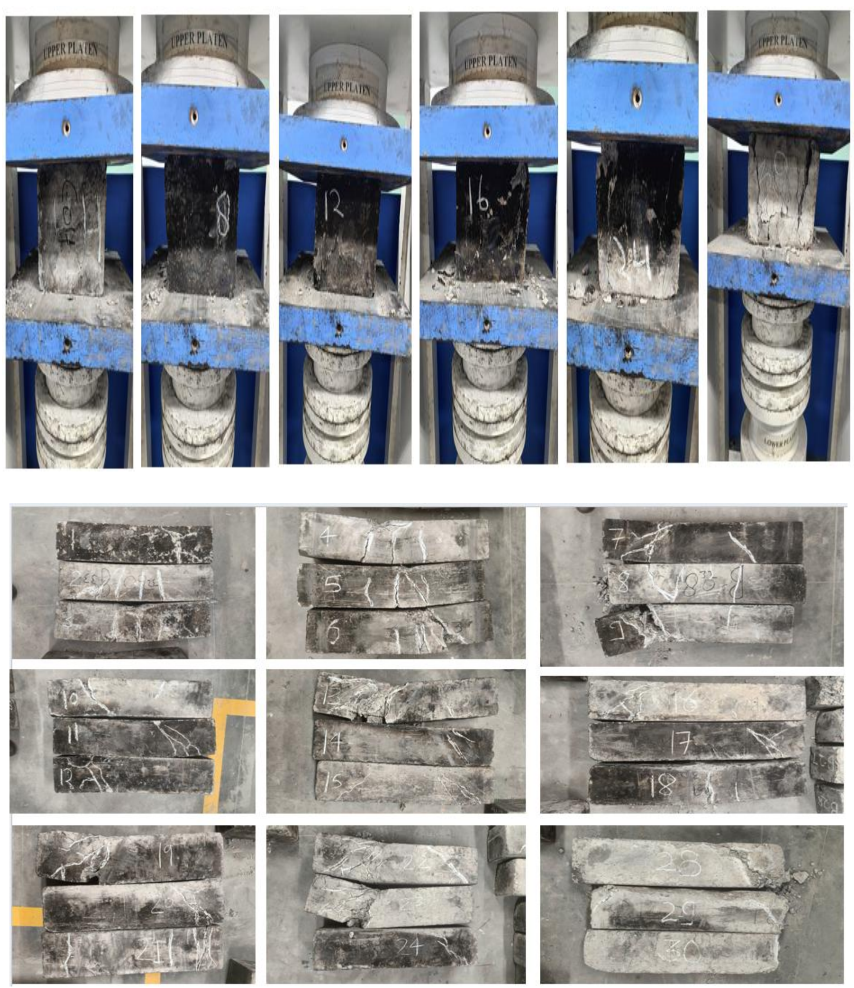

Fig. 5 Destructive strength testing of the cube and beam

2.7. Microscopic Analysis (SEM-EDS)

Small samples of concrete were extracted from select specimens (cubes and beams) after testing to observe microstructural changes. Pieces from the interior (avoiding surface carbonation layers) were taken from an unheated control, and from specimens heated to 200 °C and 1050 °C (one each cooling method). These samples were vacuum dried and then examined under a Scanning Electron Microscope.

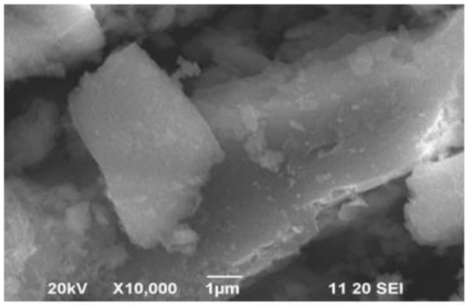

200-250 Degree Celsius

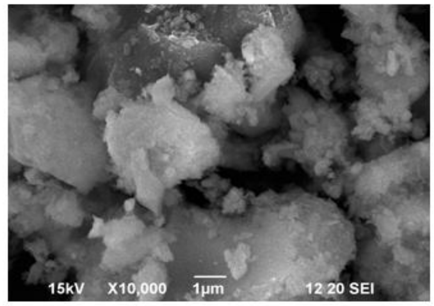

400-450 Degree Celsius

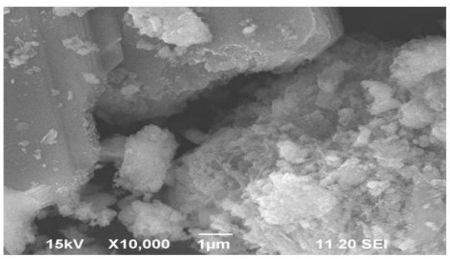

600-650 Degree Celsius

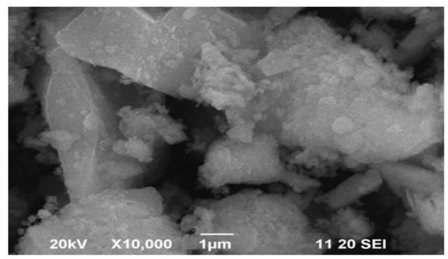

800-850 Degree Celsius

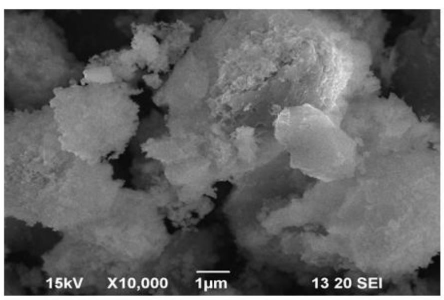

1000-1050 Degree Celsius

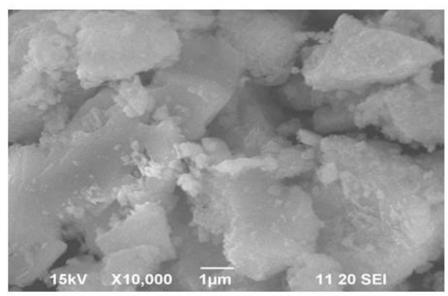

Room Temperature

Fig. 6 SEM for differnent temperature (water cooling)

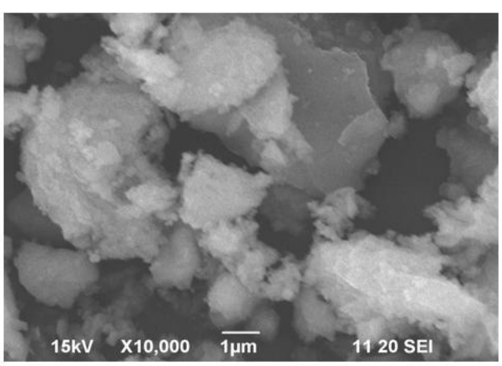

200-250 Degree Celsius

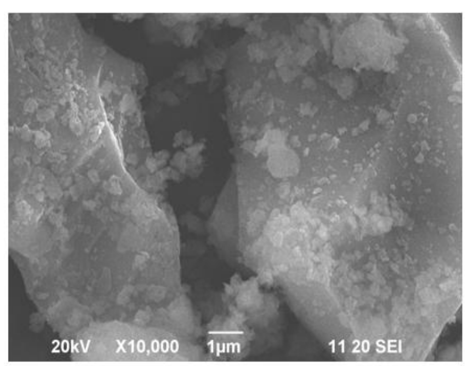

400-450 Degree Celsius

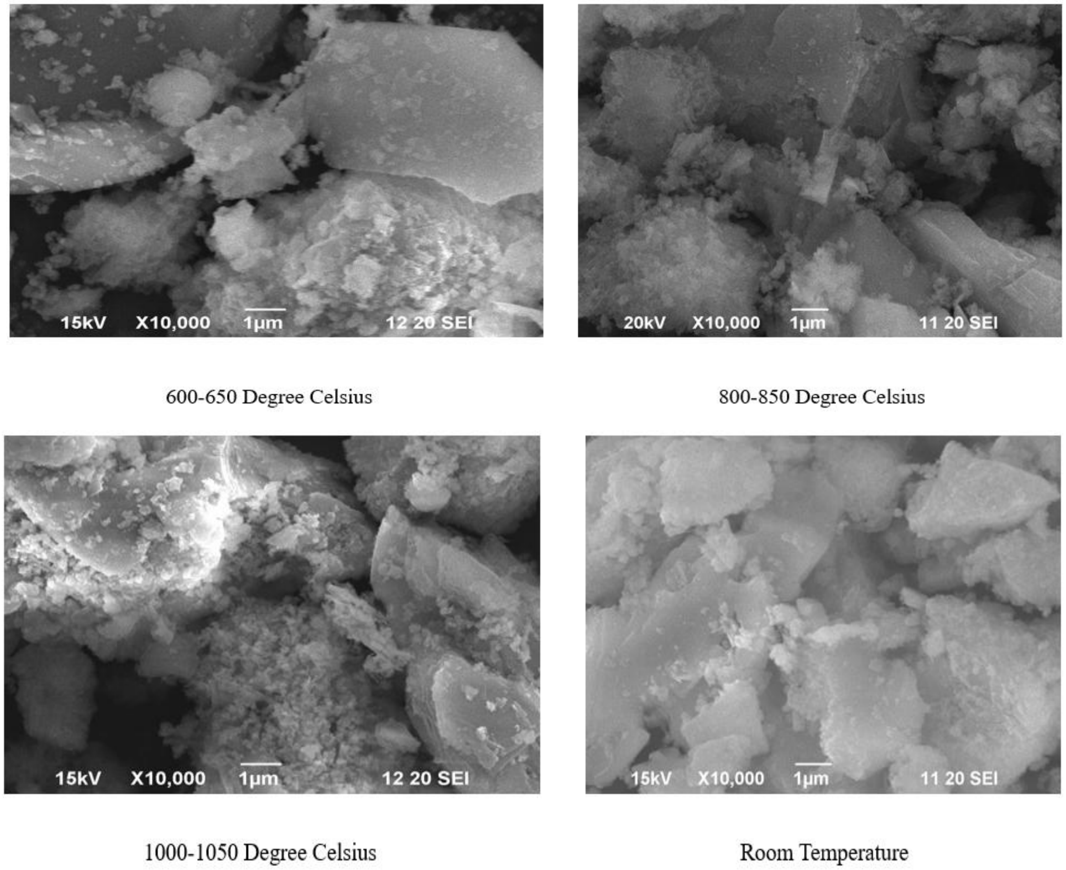

Fig. 7 SEM for different temperatures (air cooling)

Looking closely with the SEM, at high magnification, at where the cement and the aggregates meet, there were noticeable cracks, voids and how the material's structure was changing. Moreover, using Energy Dispersive X-ray Spectroscopy (EDS), not with absolute precision, how much of each element was present, looking for changes like a decrease in calcium hydroxide (portlandite) or the formation of new, re-formed materials - as Figures 6 to 9 illustrate.

This confirmed the chemical breakdown going on (for example, calcium oxide forming after the portlandite disappears), and this breakdown is what causes the loss of strength.

Due to space constraints, detailed SEM-EDS results are summarized qualitatively in this paper. The Energy Dispersive X-ray Spectroscopy (EDS) indicates the following:

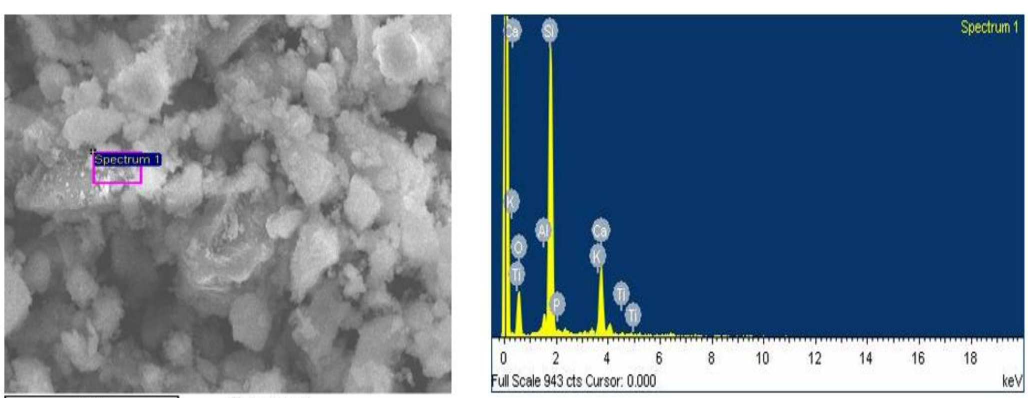

Fig. 8(a) 200-250 Degree celsius water cooling

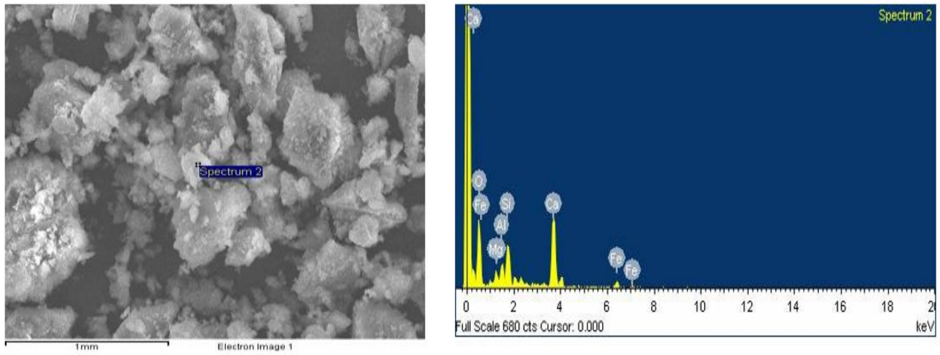

Fig. 8(b) 400-450 Degree celsius water cooling

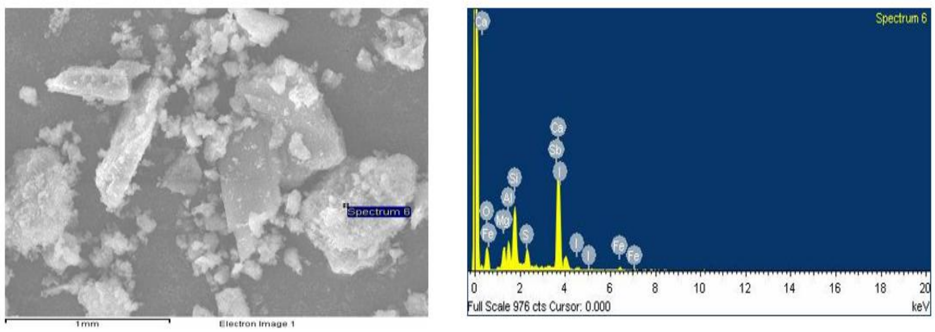

Fig. 8(c) 600-650 Degree celsius water cooling

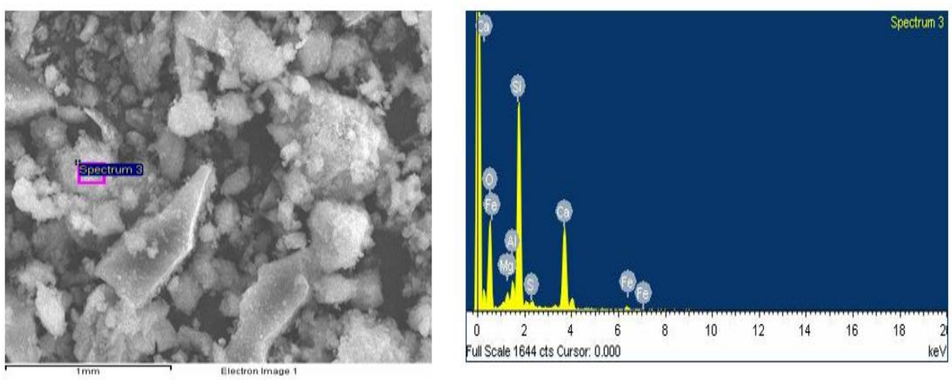

Fig. 8(d) 800-850 Degree celsius water cooling

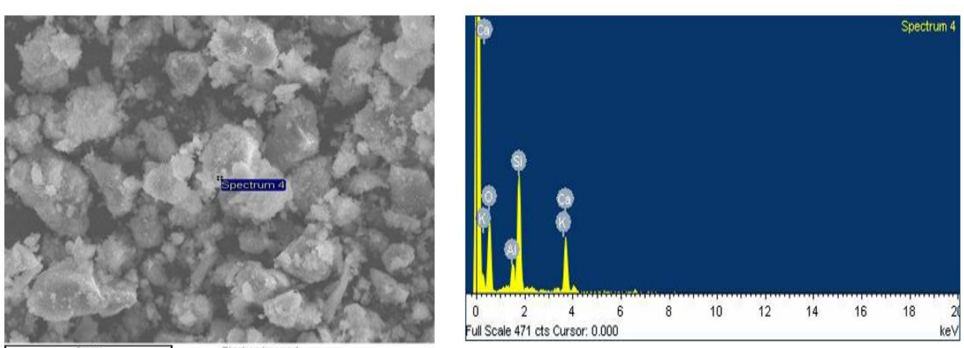

Fig. 8(e) 1000-1050 Degree celsius water cooling.

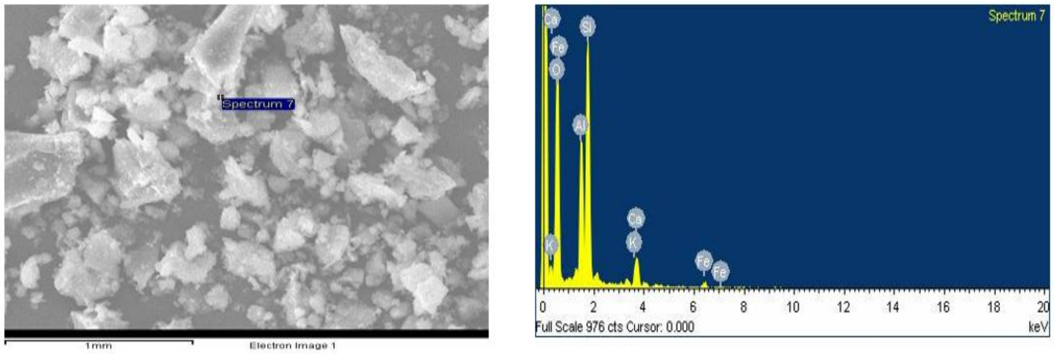

Fig. 9(a) 200-250 Degree celsius air cooling

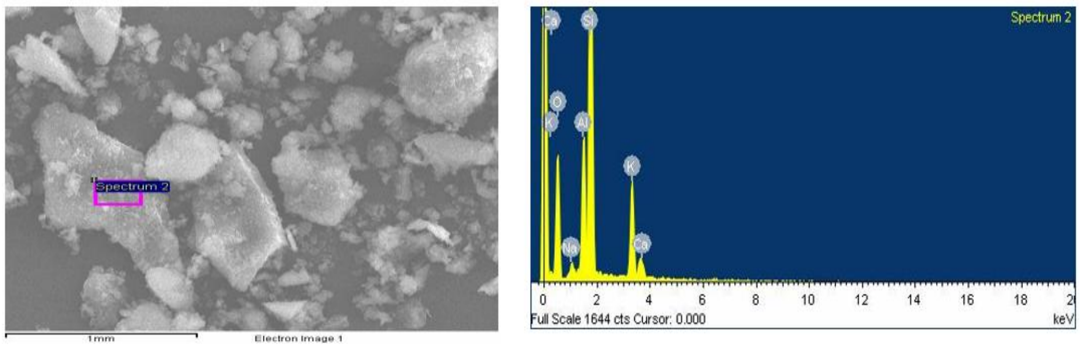

Fig. 9(b) 400-450 Degree celsius air cooling

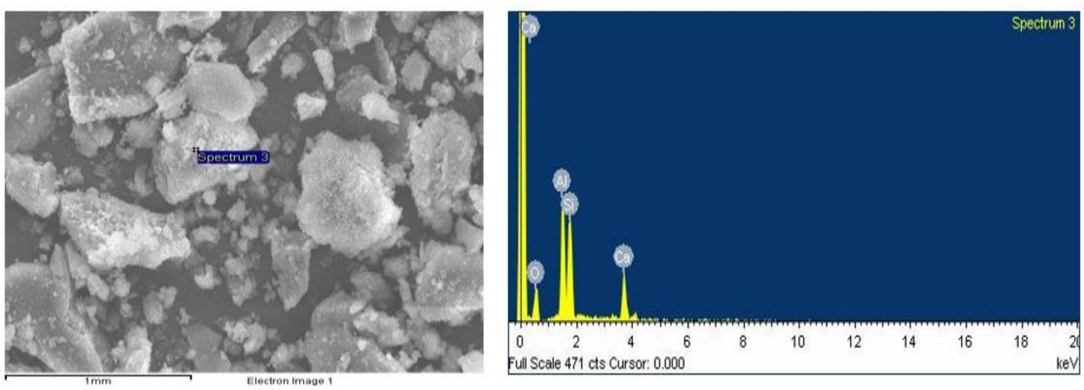

Fig. 9(c) 600-650 Degree celsius air cooling

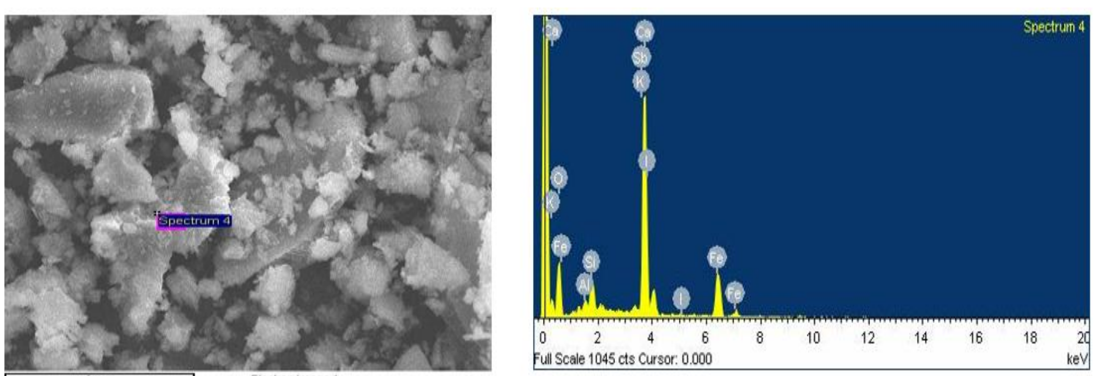

Fig. 9(d) 800-850 Degree celsius air cooling

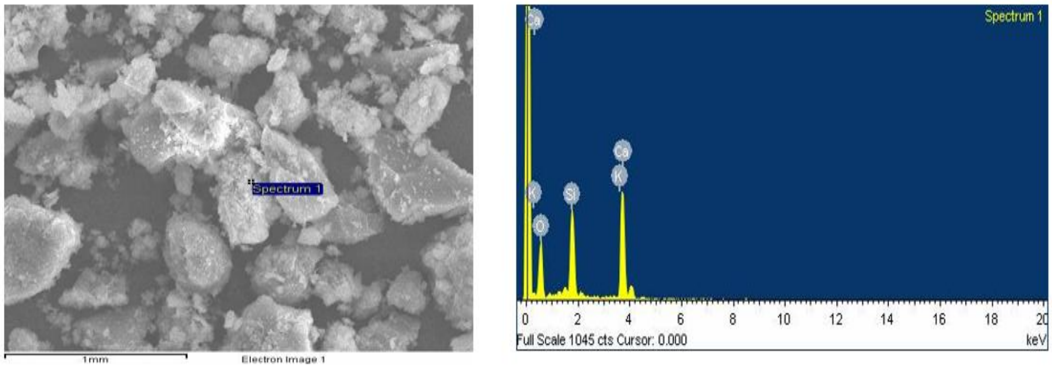

Fig. 9(e) 1000-1050 Degree celsius air cooling.

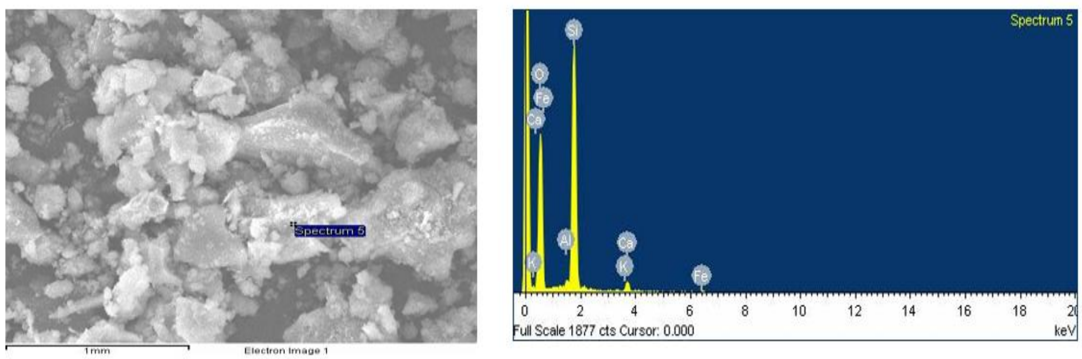

Fig. 10 Room temperature no cooling required

3. Results and Discussion

3.1. Thermal Damage: Weight Loss and Dimensional Changes

The exposure to elevated temperatures caused progressive mass loss in the concrete specimens due to moisture evaporation and dehydration of cement hydrates [22].

Figure 11 validates the average percentage weight loss of the specimens (for each temperature range) measured after cooling [16, 18, 20, 23, 24].

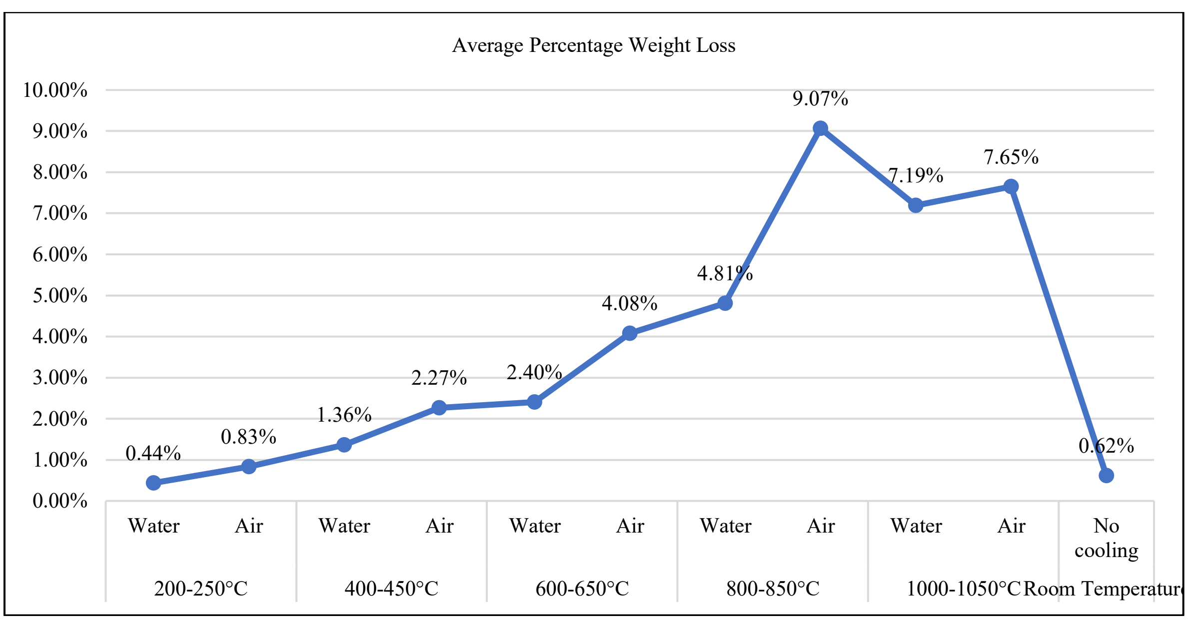

Fig. 11 Weight loss vs exposure temperature (Water- Cooled vs. air cooled)

The weight loss increased with peak temperature in a roughly exponential trend. At the lowest exposure of 200-250 °C, weight loss was minimal - around 0.4% for water-cooled cubes versus 0.8% for air-cooled (relative to original weight). This corresponds primarily to the release of free water in pores. At 400-450 °C, losses remained low (1-2%) but air-cooled samples lost nearly double the mass of water-cooled ones, suggesting that slower cooling allows slightly more dehydration (since the concrete stays hot longer) [2, 22, 25-27]. By 600-650 °C, weight loss became noticeable: 2.4% (water) vs 4.1% (air). In contrast, water quenching may trap some moisture or cause a densification of near-surface concrete that slightly reduces further mass loss. At 800-850 °C, the trend continued: water-cooled samples 4.8% lighter, air-cooled 9.1% lighter [24, 28]. Here, the air-cooled concrete, in addition to thermal dehydration, may have experienced some thermal cracking-induced mass loss (loss of small chips) and more complete decomposition of calcium hydroxide and C-S-H. Interestingly, at the highest exposure of 1000-1050 °C, both cooling methods converged to about 7-7.6% weight loss. This severe heating drives off virtually all chemically bound water (which accounts for 7-10% mass in hydrated cement paste) and begins to burn off minor amounts of aggregates or any admixtures. The similar values for water and air cooling at 1000 °C suggest that once concrete is heavily degraded, the cooling rate has little additional effect on mass - essentially all possible volatiles have been expelled during heating. The room-temperature control samples showed a negligible 0.6% mass change (some slight drying shrinkage since casting), confirming that the weight losses at high temperature are indeed due to thermal effects.

Mass loss increases sharply with temperature, reflecting moisture and dehydration. Samples that cooled in air consistently lost more weight than those water-cooled between 200 and 850°C, which suggests that being heated for longer makes more water evaporate. By 1000°C, though, both had lost about the same amount of weight (7-8%), meaning almost all the water had gone from both [28].

Alongside losing weight, the samples also changed size, but not by a lot. For the cube shaped samples, the 150mm sides changed in length by no more than plus or minus 0.6% at any of the temperatures.

The concrete beams also showed very little overall stretching or compression along their 700mm length (called dimension L1). Up to 600°C, the change was between 0.0% and 0.3%, and did not obviously favour one cooling method over the other. At 800-850°C and 1000°C, air-cooled beams tended to expand more than water-cooled ones [24].

3.2. Ultrasonic Pulse Velocity (UPV) Evaluation

A strong correlation was observed between UPV and residual compressive strength. The general trend observed was a decrease in UPV with increasing temperature, corresponding to increased cracking and defect content [14, 29, 30]. For the 150 mm path in cubes, the transit time of the ultrasonic pulse increased progressively as temperatures increases. At ambient conditions, the initial transit time was around 34-35 µs (indicates good quality concrete). After exposure to 200-250 °C, transit times were only slightly higher, than inculcates a marginal drop in UPV. After being heated to 400-450°C, more obvious changes showed up. Water-cooled cubes had a transit time of 42 µs for the UPV test, compared to 45 µs on average for the air-cooled cubes. This means the air-cooled cubes had suffered more internal damage by this point, probably because the slower cooling gave more opportunity for tiny cracks to grow. At 600 °C, the difference persisted (water 57 µs vs air 62 µs). The velocity in air-cooled concrete dropped to roughly half its original value (e.g. 2400 m/s), whereas water-cooled was slightly better (2650 m/s) [15, 31]. This suggests that some internal cracks in water-quenched cubes were “frozen” in place before growing as large as those in air-cooled cubes. At 800-850 °C, the UPV deteriorated severely. Many cubes had extensive cracking such that consistent UPV readings were difficult - transit times spiked to 140-160 µs (if a path could be found at all). The material at this stage is heavily damaged, with a velocity under 1000 m/s (essentially behaving like a granular porous solid). Both cooling methods yielded extremely long travel times, though water-cooled cubes sometimes showed slightly lower transit times than air (e.g. 139 µs vs 157 µs on average), indicating marginally less damage in the quenched specimens. At 1000 °C, the concrete cubes were so cracked that an ultrasonic pulse could not be propagated through the 150 mm length in most cases - effectively, no UPV signal could be obtained (transit time recorded as zero signal). This corresponds to a complete loss of continuity in the material; the internal micro-crack network had become a macro-crack network separating the cube into pieces (although held together by aggregates and any residual cement). Thus, in UPV terms, the cubes had lost all ability to transmit stress waves at the highest temperature, corroborating the drastic strength loss [30, 32-34].

For the RC beams, UPV measurements yielded additional information due to the two path lengths. Along the short 150 mm depth, trends were similar to cubes. Along the full 700 mm span, the results dramatically illustrate the onset of structural-level cracking. At 200-250 °C, beams transmitted the pulse along 700 mm with little issue - transit times were 230-250 µs (baseline was 210-230 µs before heating, corresponding to 3100 m/s velocity over that length). There was an interesting observation: water-cooled beams showed a higher increase in long-path transit time at 200 °C than air-cooled (e.g. +30 µs vs +20 µs), which means the quenching introduced some early cracking or debonding that slightly impeded wave travel. However, as the temperature increased, the trend reversed. By 400-450 °C and 600-650 °C, the air-cooled beams exhibited much larger increases in 700 mm transit time compared to water-cooled. For instance, at

600 °C, a representative water-cooled beam had a long-path time of 376 µs, whereas an air-cooled counterpart had 553 µs - the latter is about 47% longer, implying significantly more internal damage or possibly that the signal took slower indirect routes around cracks.

In fact, one air-cooled beam at 600 °C had no discernible through-signal, suggesting a major crack fully separating the span. Figure 2 plots the UPV transit times before vs. after fire for the beam specimens, highlighting these differences. By 800 °C, neither cooling regime could preserve a through-path: both water- and air-cooled beams failed to transmit a 700 mm signal (the pulse was completely attenuated by large cracks around mid-span).

The 150 mm local UPV still registered (e.g. 106 µs water vs 130 µs air at 800 °C, indicating water-cooled had slightly less local damage), but along the span, the concrete was effectively broken. The beams could not transmit the UPV signal over 700mm at 1000°C, and even the 150mm UPV was extremely slow (between 300 and 400 µs). These UPV results confirm that between 800 and 1000°C, the material basically falls apart.

They also show that the way the material is cooled affects the damage at intermediate temperatures: in the 400-800°C range, water cooling generally meant a smaller increase in UPV than air cooling. However, at 200°C, water cooling caused marginal cracking immediately, and this showed in a slightly higher UPV reduction than the air-cooled cubes at that single temperature. Overall, the UPV assessment correlates with the strength findings and provides a non-destructive indicator: higher transit times (lower velocities) correspond to lower residual strength, as discussed next [14, 29, 35].

3.3. Residual Compressive and Flexural Strength

The compressive strength of concrete cubes after exposure and cooling showed a clear decline with temperature, as summarized in Figure 12. At 28-day ambient conditions, the average cube strength was 32 MPa. After heating to 200-250 °C, the residual compressive strength was only marginally reduced: air-cooled cubes averaged 31.5 MPa, which is slightly above the initial strength, whereas water-cooled cubes averaged 30.5 MPa [18, 36, 37]. By 400-450°C, there was a significant strength reduction [5]. Water-cooled cubes averaged 25.4 MPa (80% of their original strength), and the air-cooled ones were around 26.4 MPa. This 20% strength loss is linked to portlandite drying and early changes in the C-S-H material at about 400°C. Again, the air-cooled cubes retained a little more strength at 400°C, which is consistent with water cooling causing more small cracks, even though they lost less weight. Between 600 and 650°C, both cooling methods left roughly half the original strength remaining. Water-cooled cubes averaged 25.4 MPa, and air-cooled cubes dropped to 23.9 MPa. In this instance, the water-cooled cubes performed better. This reversal indicates that above 500°C, the air-cooled material suffers more and more damage to the 'cementitious matrix' holding it all together, but quickly cooling with water might help to keep some strength by rapidly reducing the temperature. However, at 600°C, the remaining strengths are very similar (75% of the original for both). A big drop in strength occurred at 800-850°C: the strength fell to 21-22 MPa (65% down from the original). Air-cooled cubes averaged 22.4 MPa, and water-cooled 21.3 MPa, so the air-cooled cubes were stronger at this point. However, with so much cracking at this stage, this small difference could be just a random variation. Finally, at the extreme temperature of 1000-1050°C, the cubes had hardly any strength at all [7, 37-39].

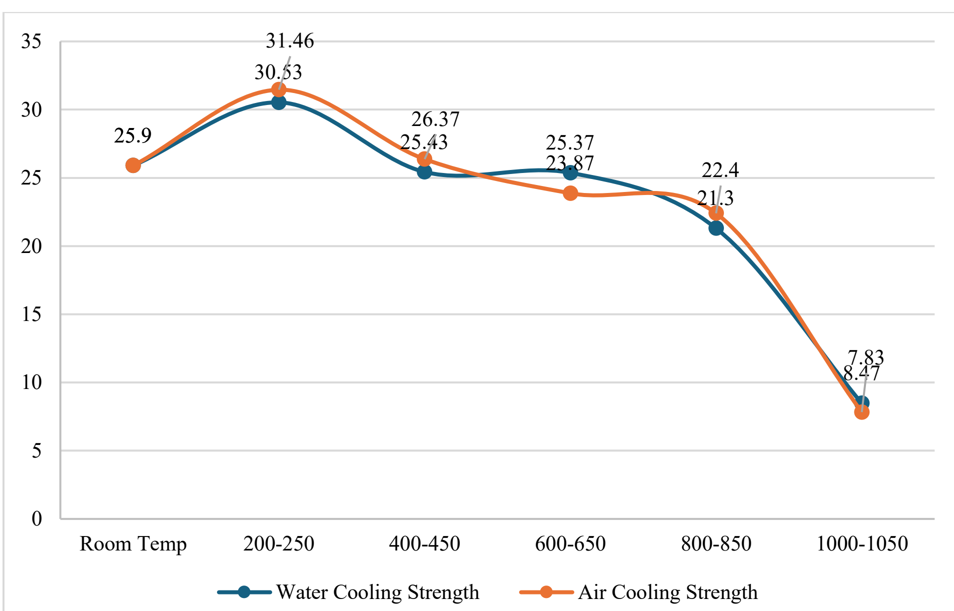

Fig. 12 Peak temperature Vs residual compressive strength of concrete cubes, comparing air vs. water cooling

The water-cooled concrete cubes managed around 8.5 MPa, and the air-cooled ones about 7.8 MPa. Both of these strengths are only about 25% of what they originally were. The water-cooled cubes being stronger (+0.6 MPa) might be because when they were quickly cooled (quenched), some of the calcium oxide turned back into calcium hydroxide, which provides marginal matrix adhesion. Up to 200°C, the concrete held onto most of its strength, but by 400°C, it had lost twenty percent. Then, between 600 and 800°C, it rapidly deteriorates, and at 1000°C is down to only twenty-five percent of its original strength. At 200, 400 and 800°C, the cubes cooled in air were stronger, while at 600 and 1000°C, those cooled in water were better. The difference was not large, remaining under 1.5 MPa. Concrete's strength really begins to give way in the 600-800°C range.

Before 400°C, both its compressive and bending strengths remained reasonably good (80 % percent of the original), according to another research. However, by 600-800°C, it had lost around half its strength. Then, the cooling method impacts compressive and bending strengths in different ways. Air cooling gave marginally more residual strength for the plain concrete cubes at 200, 400 and 800°C and water cooling at 600 and 1000°C, but these differences were fairly small (within 5 % of the strength) and were not consistent. This suggests cooling does not consistently change the strength in compression until it reaches high temperatures, and then quickly cooling might keep more strength in the concrete [5]. After 200-250 °C exposure, the air-cooled beams actually showed a slight increase in strength: they sustained a flexural stress of 6.46 MPa, marginally higher than the original. This could be attributed to the drying of concrete (increasing its tensile strength somewhat) and the fact that steel reinforcement at 200 °C experiences only mild thermal softening (and once cooled, steel regains its yield strength fully for such a low temperature). On the other hand, the water-quenched beams at 200 °C had an average residual flexural strength of 5.60 MPa, about 15% lower than the original. The likely cause is the thermal shock inducing microcracks at the concrete-steel interface and within the concrete tension zone, thereby reducing the beam's cracking moment and stiffness. Thus, at low temperature, air cooling was beneficial, and water cooling caused a drop in beam strength (consistent with the earlier UPV observation at 200 °C).

When heated to 400-450 °C, the beams exhibited more damage but an interesting crossover: water-cooled beams showed 5.2 MPa flexural strength, slightly higher than the 5.0 MPa for air-cooled. The air-cooled beam strength had now fallen to 75% of its original, whereas the water-cooled was around 80% of its original. This suggests that by 400 °C, the extended heat exposure for air cooling (and potential additional creep of steel at high temperature) outweighed the negative effects of thermal shock. Water cooling may also have helped the steel reinforcement recover its strength more quickly (the rapid temperature drop could prevent prolonged metallurgical effects on steel). Additionally, quenching might induce compressive surface stresses beneficial in flexure (though it likely cracks the surface, so this point is speculative). In any case, from 400 °C onward, the water-cooled beams retained equal or greater strength than air-cooled in our tests. At 600-650 °C, water-cooled beams were at 5.25 MPa vs air-cooled 4.98 MPa. The gap widened further at 800-850 °C: water-cooled 5.16 MPa, air-cooled 4.61 MPa. Moreover, at the highest 1000 °C level, water-cooled beams still managed 3.7 MPa, while air-cooled beams dropped to 2.1 MPa, as shown in Figure 13. That is a substantial difference (water-cooled retaining 54% of its original flexural strength, air-cooled only 30% at 1000 °C).

It appears that in the beams, rapid cooling benefited the residual capacity at high temperatures, perhaps by preventing additional time for the steel to yield or for cracks to propagate. Water quenching might also rehydrate some of the dehydrated cement paste around the reinforcement, improving the bond or adding solidity (e.g. CaO reconverting to $Ca(OH)_2$ and filling cracks). In contrast, air-cooled beams cooled slowly, allowing gravity and thermal gradients to sometimes cause more cracking (one air-cooled beam at 800 °C failed under its own weight during cooling, whereas all water-quenched beams remained intact until testing) [18, 21, 34, 36].

The way the reinforced concrete beams bent (flexural strength) was slightly different, as the steel inside them and how well the concrete and steel work together both affect how much they can bend. Initially, before heating, the beams could bend until they broke at an average of 6.5-6.9 MPa - about what you would expect from 32 MPa concrete. At 200°C, the air-cooled beams were stronger than their original strength (6.5 MPa), while the water-cooled ones dropped to 5.6 MPa because the rapid cooling created small cracks inside [40]. Once the temperature went above 400°C, the water-cooled beams were always stronger than the air-cooled ones, and the difference got bigger as it got hotter. By 1000°C, the water-cooled beams held 3.7 MPa, compared to only 2.1 MPa for the air-cooled ones (+1.6 MPa difference) - showing they were much better at still carrying a load with fast cooling.

Any extra damage from the quick cooling at moderate temperatures was pretty much cancelled out by the concrete being less damaged by the heat. However, with the bending of the beams, the differences were bigger and more predictable: the water-cooled beams weren't as good at the lowest temperature (because of thermal shock), but were better at higher temperatures, and by 1000°C were 60-70% stronger. This indicates that how a structure behaves, especially with steel in it, can be more affected by cooling. It is probably because of how well the steel and concrete stick together and how much stiffness is left in the concrete on the tension side. The air-cooled beams might have had the steel pull away more (as the connection stayed hot for longer and more water moved around), whereas the quick cooling could have 'frozen' the connection in place (though with some cracking). After cooling, the steel in both sets of beams is back to normal temperature - any difference in how the beams can bend comes from the concrete and the bond. The higher strength of water-cooled beams at high temperatures implies a stronger bond between the steel and concrete, or less cracking around the steel, compared to the slowly cooled beams, which likely have wider cracks. As other investigations have indicated, how strongly the steel and concrete remain connected after a fire is a major concern during fires, and both slow cooling and high temperatures can substantially reduce that connection. Quickly cooling it might reduce the time for this to happen.

Lastly, even though the water-cooled beams were stronger than the air-cooled ones at 800-1000°C, those strengths (3-5 MPa bending stress) are really low. In reality, neither of them could hold very much weight compared to how they used to, so they would need a lot of repairs or replacing after a fire. However, from a materials science point of view, the difference in strengths validates that water quenching did not completely ruin the concrete.

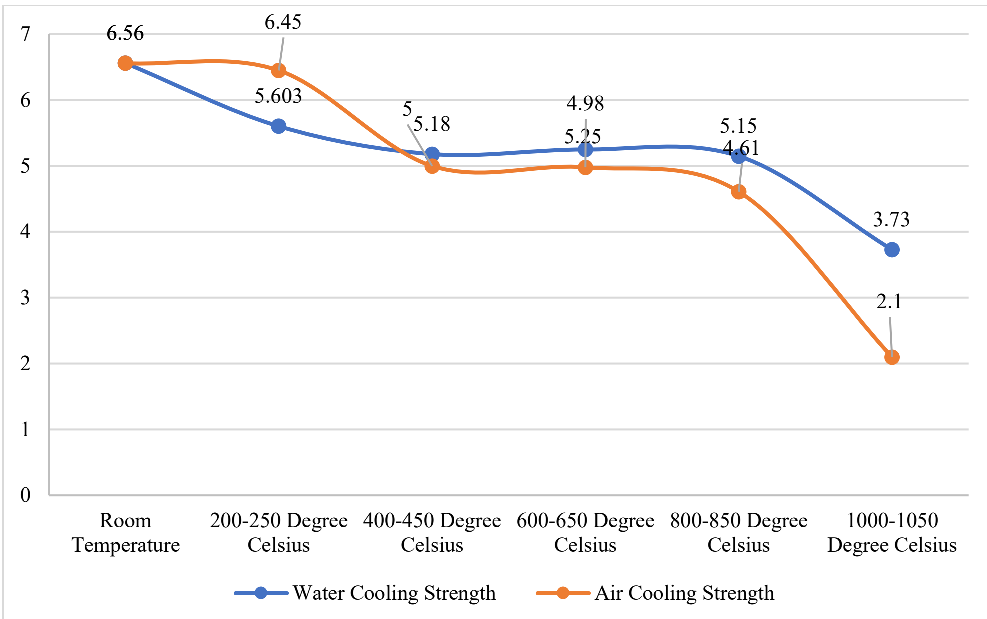

Fig. 13 Residual flexural strength of rc beams vs exposure temperature for different cooling methods

3.4. Microstructural Analysis (SEM-EDS Findings)

The increase in microcrack density observed in SEM images at elevated temperatures directly correlates with the reduction in compressive strength and UPV values, confirming the progressive deterioration of the concrete matrix. Looking at the concrete with a microscope confirmed that extensively tiny cracks formed and the makeup of the concrete altered at each temperature. In unheated control concrete, SEM images showed a dense cement paste with evenly distributed fine pores and good bonding at the aggregate-paste interface. After exposure to 600 °C, the SEM of air-cooled samples showed numerous micro-cracks in the paste, often lining the edges of aggregate particles (interfacial transition zone cracks) [41, 42]. Pores were observed to have grown in size - likely due to the loss of bound water and coalescence of smaller pores. There was evidence of ettringite and portlandite depletion, as EDS spectra indicated a reduction in calcium hydroxide peaks [41]. The micro-cracks at this stage were sub-millimeter width but widespread, explaining the moderate strength loss (about 50%). Water-cooled samples at 600 °C exhibited a broadly similar crack pattern, but some cracks appeared less continuous (perhaps some were arrested by the quench). EDS on quenched samples also sometimes detected reprecipitated $Ca(OH)_2$ in cracks (from lime reacting with quench water), which could contribute to the slightly higher compressive strength seen in water-cooled cubes at 600 °C [43-45].

By 1000 °C, the microstructure was dramatically altered. SEM images showed extensive cracking and voids - the cement paste had largely disintegrated into a network of rubble. Aggregate surfaces were cracked and, in some cases, showed a thermal alteration layer (e.g. quartz aggregates had undergone phase transitions causing fracturing) [46-48]. The paste was full of lime particles and possibly β-C_2S (belite) crystals as C-S-H completely decomposed. EDS confirmed the absence of structural water: virtually no hydroxide remained, and only oxides of Ca, Si, etc. were present. Interestingly, the water-quenched specimen at 1000 °C had some fissures lined with portlandite - a result of CaO formed during heating subsequently rehydrating when dunked in water. This "secondary" portlandite likely did not restore strength significantly (as overall the structure was cracked), but it indicates that quenching can cause chemical changes (rehydration) in addition to mechanical cracking. The air-cooled specimen, in contrast, had no portlandite, but a fluffier morphology of CaO and possibly $CaCO_3$ (from slight carbonation when cooling in air). These details about the concrete's inner structure strongly suggest that pouring water on hot concrete can actually repair some of the damage (by reabsorbing water), even though it also causes quick, shrinking cracks from the sudden temperature drop. Overall, in our tests, the beams heated to high temperatures benefited from this, and cubes were about the same as they would have been, as previously discussed [45, 46, 48-50].

3.5. Predictive Modeling and Statistical Correlation

To establish a quantitative relationship between thermal exposure, internal damage, and residual mechanical performance, a regression-based predictive model was developed using the experimental dataset. The model correlates residual compressive strength with peak temperature and Ultrasonic Pulse Velocity (UPV), which serves as a non-destructive indicator of internal integrity.

$$Fc = 34.5 - 0.018T + 0.0042V$$

where:

(Fc) = Residual compressive strength (MPa),

(T) = Exposure temperature (°C),

(V) = Ultrasonic Pulse Velocity (m/s).

The model demonstrates that temperature and UPV jointly govern the degradation behavior of concrete. The negative coefficient associated with temperature confirms that thermal exposure is the primary driver of strength reduction. This occurs due to dehydration of cement hydrates and progressive microcracking. Specifically, the model indicates a reduction of approximately 1.8 MPa in compressive strength for every 100°C increase in temperature. The positive coefficient of UPV highlights its effectiveness as a proxy for internal structural integrity. Higher UPV values correspond to denser and less damaged concrete, resulting in improved residual strength. The predictive capability of the model was validated by comparing estimated values with experimental results (yielding an overall prediction accuracy exceeding 90%). This level of agreement confirms the validation of the model for practical engineering applications.

In contrast, UPV provides greater discriminatory capability in the moderate temperature range (200-600°C). The internal damage is not yet macroscopically visible but significantly affects material stiffness and integrity. The developed model offers a practical framework for post-fire assessment of reinforced concrete structures. By combining easily measurable UPV data with estimated exposure temperature, engineers can reliably predict residual strength without resorting to destructive testing. This results in the rapid structural evaluation and decision-making following fire incidents. However, it should be noted that the model is empirical and is strictly valid within the investigated temperature range (25°C to 1050°C). Further refinement using larger datasets and the incorporation of additional parameters such as cooling rate, moisture condition, and reinforcement ratio may enhance predictive accuracy.

Overall, the integration of experimental results with predictive modeling significantly enhances the analytical depth and practical relevance of the present study. This addresses a critical gap in post-fire structural assessment methodologies.

4. Conclusion

This study presents a comprehensive experimental investigation into the effects of elevated temperature exposure and cooling regimes on the residual mechanical performance of reinforced concrete members. The results confirm that thermal degradation significantly affects both compressive and flexural strength. The critical deterioration occurs beyond 600°C due to microstructural damage, including dehydration of cement hydrates, increased porosity, and extensive microcracking.

The comparison between cooling methods revealed that water quenching, despite inducing minor thermal shock at lower temperatures. In contrast, air-cooled specimens exhibited greater internal deterioration due to extended exposure to elevated temperatures during gradual cooling.

Ultrasonic Pulse Velocity (UPV) measurements demonstrated a strong correlation with residual strength and internal damage. This validates their effectiveness as a reliable non-destructive evaluation tool for post-fire assessment. Microstructural analysis using SEM-EDS further confirms the progressive degradation mechanisms. A regression-based predictive model was successfully developed to estimate residual compressive strength as a function of temperature and UPV. The model achieved prediction accuracy exceeding 90% and provides a practical framework for rapid, non-destructive assessment of fire-damaged concrete structures.

Overall, the integration of experimental observations, microstructural insights, and predictive modeling enhances the scientific depth and practical applicability of the study, offering valuable guidance for structural evaluation and rehabilitation following fire exposure.

Acknowledgement

The authors have not received any funding. The authors thank Integral University, Lucknow, for providing all necessary facilities for carrying out the research. MCN: IU/R&D/2026-MCN0004378.

References

[1] Musa Adamu, Yasser E. Ibrahim, and Hani Alanazi, “Evaluating the Influence of Elevated Temperature on Compressive Strength of Date-Palm-Fiber-Reinforced Concrete using Response Surface Methodology,” *Materials*, vol. 15, no. 22, pp. 1-25, 2022. [CrossRef] [Google Scholar] [Publisher Link]

[2] Eneye A. Ibrahim et al., “Assessing Post-Fire Damage in Concrete Structures: A Comprehensive Review,” *Buildings*, vol. 15, no. 3, pp. 1-21, 2025. [CrossRef] [Google Scholar] [Publisher Link]

[3] Muhammad Noman et al., “Effects of Low-Cost Repair Techniques on Restoration of Mechanical Properties of Fire-Damaged Concrete,” *Frontiers in Materials*, vol. 8, pp. 1-14, 2022. [CrossRef] [Google Scholar] [Publisher Link]

[4] Mariam F. Ghazy, Metwally A. Abd Elaty, and Nagat M. Zalhaf, “Performance of Normal Strength Concrete Slab Strengthened with High-Performance Concrete After Exposure to Elevated Temperature,” *Fire Technology*, vol. 59, no. 5, pp. 2415-2453, 2023. [CrossRef] [Google Scholar] [Publisher Link]

[5] Alan Saeed Abdulrahman, and Mohamed Raouf Abdul Kadir, “Behavior and Flexural Strength of Fire Damaged High Strength Reinforced Rectangular Concrete Beams after Strengthening with CFRP Laminates,” *Ain Shams Engineering Journal*, vol. 13, no. 6, pp. 1-14, 2022. [CrossRef] [Google Scholar] [Publisher Link]

[6] Jakub Vůjtěch et al., “Strengthening, Lifetime Extension, and Monitoring of a Deficient Steel-Concrete Composite Roadway Bridge using Iron-based Shape Memory Alloys,” *Engineering Structures*, vol. 323, pp. 1-15, 2025. [CrossRef] [Google Scholar] [Publisher Link]

[7] Kateřina Horníková, and Marek Foglar, “Compressive Strength of Various Types of Concrete Exposed to Elevated Temperature,” *Solid State Phenomena*, vol. 309, pp. 62-67, 2020. [CrossRef] [Google Scholar] [Publisher Link]

[8] Fu Ping Cheng, V.K.R. Kodur, and Tien Chih Wanget al., “Stress-Strain Curves for High Strength Concrete at Elevated Temperatures,” *Journal of Materials in Civil Engineering*, vol. 16, no. 1, pp. 84-90, 2004. [Google Scholar] [Publisher Link]

[9] E. Annerel, and L. Taerwe, “Revealing the Temperature History in Concrete after Fire Exposure by Microscopic Analysis,” *Cement and Concrete Research*, vol. 39, no. 12, pp. 1239-1249, 2009. [CrossRef] [Google Scholar] [Publisher Link]

[10] Saeid Hesami et al., “Investigating the Rheological Properties and Microstructural Analysis of Nano-Expanded Perlite Modified Asphalt Binder,” *Case Studies in Construction Materials*, vol. 22, pp. 1-20, 2025. [CrossRef] [Google Scholar] [Publisher Link]

[11] Heloina Nogueira da Costa, Antônio Eduardo Bezerra Cabral, and Ricardo Emílio Ferreira Quevedo Nogueiraet al., “Alkali-Activated Pastes by Basic Oxygen Furnace slag and Fly ash: Mechanical and Microstructural Analysis,” *Case Studies in Construction Materials*, vol. 22, pp. 1-16, 2025. [CrossRef] [Google Scholar] [Publisher Link]

[12] Bing Li, Wenbin Zheng, and Yang Zhang, “Study on the Compressive Stress-Strain Curve and Performance of Low-Slump Polypropylene Fiber Concrete after High Temperature,” *Applied Sciences*, vol. 13, no. 12, pp. 1-25, 2023. [CrossRef] [Google Scholar] [Publisher Link]

[13] Wenxiao Lu et al., “Evaluation of Mechanical Properties and Cracking Resistance of Shrinkage-Compensating Concrete Reinforced by Expansive Agents with Polypropylene Fibers,” *Case Studies in Construction Materials*, vol. 22, pp. 1-14, 2025. [CrossRef] [Google Scholar] [Publisher Link]

[14] J. Wróblewska et al., “Application of Ultrasonic Pulse Velocity Test to Concrete Assessment in Structures after Fire,” *Archives of Civil Engineering*, vol. 67, no. 3, pp. 395-413, 2021. [CrossRef] [Google Scholar]

[15] Wonchang Kim et al., “A Study on Correlation between Ultrasonic Pulse Velocity Method and Coarse Aggregate for Estimating Residual Modulus of Elasticity of Concrete Exposed to High Temperatures,” *Applied Sciences*, vol. 12, no. 13, pp. 1-15, 2022. [CrossRef] [Google Scholar] [Publisher Link]

[16] A. Ferhat Bingöl, and Rüstem Gül, “Effect of Elevated Temperatures and Cooling Regimes on Normal Strength Concrete,” *Fire and Materials*, vol. 33, no. 2, pp. 79-88, 2009. [CrossRef] [Google Scholar] [Publisher Link]

[17] M.M. Shoaib, S.A. Ahmed, and M.M. Balaha, “Effect of Fire and Cooling Mode on the Properties of Slag Mortars,” *Cement and Concrete Research*, vol. 31, no. 11, pp. 1533-1538, 2001. [CrossRef] [Google Scholar] [Publisher Link]

[18] Sándor Fehérvári, “Effect of Cooling Methods on the Residual Properties of Concrete Exposed to Elevated Temperature,” *Results in Engineering*, vol. 16, pp. 1-11, 2022. [CrossRef] [Google Scholar] [Publisher Link]

[19] Mehmet Burhan Karakoç, “Effect of Cooling Regimes on Compressive Strength of Concrete with Lightweight Aggregate Exposed to High Temperature,” *Construction and Building Materials*, vol. 41, pp. 21-25, 2013. [CrossRef] [Google Scholar] [Publisher Link]

[20] Marian Abramowicz, and Robert Kowalski, “The Influence of Short Time Water Cooling on the Mechanical Properties of Concrete Heated up to High Temperature,” *Journal of Civil Engineering and Management*, vol. 11, no. 2, pp. 85-90, 2005. [CrossRef] [Google Scholar] [Publisher Link]

[21] A.S.M. Abdul Awal, I.A. Shehu, and Mohammad Ismail, “Effect of Cooling Regime on the Residual Performance of High-Volume Palm Oil Fuel Ash Concrete Exposed to High Temperatures,” *Construction and Building Materials*, vol. 98, pp. 875-883, 2015. [CrossRef] [Google Scholar] [Publisher Link]

[22] Yuqiao Cao et al., “Thermal Damage Detection in FRP-Strengthened Reinforced Concrete Structures using Ultrasonic Guided Waves,” *NDT and E International*, vol. 152, pp. 1-11, 2025. [CrossRef] [Google Scholar] [Publisher Link]

[23] Leyla Tanaçan, Halit Yaşa Ersoy, and Ümit Arpacıoğlu, "Effect of High Temperature and Cooling Conditions on Aerated Concrete Properties," *Construction and Building Materials*, vol. 23, no. 3, pp. 1240-1248, 2009. [CrossRef] [Google Scholar] [Publisher Link]

[24] A.Y. Nassif, S. Rigden, and E. Burley, "The Effects of Rapid Cooling by Water Quenching on the Stiffness Properties of Fire-Damaged Concrete," *Magazine of Concrete Research*, vol. 51, no. 4, pp. 255-261, 1999. [CrossRef] [Google Scholar] [Publisher Link]

[25] Hsuan-Chih Yang, and Yiching Lin, "A Simplified Procedure for Evaluation of Damage-Depth in Concrete Exposed to High Temperature using the Impact-Echo Method," *NDT and E International*, vol. 149, 2025. [CrossRef] [Google Scholar] [Publisher Link]

[26] Mequanent Mulugeta Alamnie, Ephrem Taddesse, and Inge Hoff, "A Study on Permanent Deformation and Fatigue Damage Interaction in Asphalt Concrete," *Construction and Building Materials*, vol. 407, pp. 1-15, 2023. [CrossRef] [Google Scholar] [Publisher Link]

[27] Qingtao Li, Guanglin Yuan, and Qianjin Shu, "Effects of Heating/Cooling on Recovery of Strength and Carbonation Resistance of Fire-Damaged Concrete," *Magazine of Concrete Research*, vol. 66, no. 18, pp. 925-936, 2014. [CrossRef] [Google Scholar] [Publisher Link]

[28] Alexandre Almeida Del Savio et al., "Experimental and Analytical Study of Temperatures Developed by the Heat of Hydration of High-Strength Self-Compacting Mass Concrete," *Case Studies in Construction Materials*, vol. 22, pp. 1-16, 2025. [CrossRef] [Google Scholar] [Publisher Link]

[29] Vinh An Le, Thi-Thanh Thao Nguyen, and Ngoc Tan Nguyen, "Investigation of Ultrasonic Pulse Velocity Reduction in Reinforced Concrete Members Exposed to High Temperature," *Journal of Materials and Engineering Structures*, vol. 9, no. 4, pp. 531-537, 2022. [Google Scholar]

[30] Mahmood Karimaei et al., "Estimating Compressive Strength of Concrete Containing Untreated Coal Waste Aggregates using Ultrasonic Pulse Velocity," *Materials*, vol. 14, no. 3, pp. 1-19, 2021. [CrossRef] [Google Scholar] [Publisher Link]

[31] Qiang Wang et al., "Evaluation Residual Compressive Strength of Tunnel Lining Concrete Structure after Fire Damage based on Ultrasonic Pulse Velocity and Shear-Wave Tomography," *Processes*, vol. 10, no. 3, pp. 1-13, 2022. [CrossRef] [Google Scholar] [Publisher Link]

[32] Yi Wang et al., "Experimental Study of Thermally Damaged Concrete under a Hygrothermal Environment by using a Combined Infrared Thermal Imaging and Ultrasonic Pulse Velocity Method," *Materials*, vol. 16, no. 3, pp. 1-19, 2023. [CrossRef] [Google Scholar] [Publisher Link]

[33] Ma. Doreen E. Candelaria, and Seong-Hoon Kee, "Evaluation of Thermal Damages of Concrete Subjected to High Temperatures using Recurrent Neural Networks for Ultrasonic Pulse Waves," *Construction and Building Materials*, vol. 407, pp. 1-17, 2023. [CrossRef] [Google Scholar] [Publisher Link]

[34] Yeol Choi et al., "Evaluation of Residual Strength with Ultrasonic Pulse Velocity Relationship for Concrete Exposed to High Temperatures," *Advances in Mechanical Engineering*, vol. 13, no. 9, pp. 1-9, 2021. [CrossRef] [Google Scholar] [Publisher Link]

[35] N. Usman et al., "Fire Resistance and Ultrasonic Testing of Rice Husk Ash Modified Foamed Concrete," *Environmental Technology and Science Journal*, vol. 15, no. 2, pp. 156-164, 2024. [CrossRef] [Google Scholar] [Publisher Link]

[36] Raad A. Al-Ameri et al., "Residual Repeated Impact Strength of Concrete Exposed to Elevated Temperatures," *Crystals*, vol. 11, no. 8, pp. 1-21, 2021. [CrossRef] [Google Scholar] [Publisher Link]

[37] Hussein M. Elsanadedy, "Residual Compressive Strength of High-Strength Concrete Exposed to Elevated Temperatures," *Advances in Materials Science and Engineering*, vol. 2019, no. 1, pp. 1-22, 2019. [CrossRef] [Google Scholar] [Publisher Link]

[38] Ivan Ivanchev, "Investigation with Non-Destructive and Destructive Methods for Assessment of Concrete Compressive Strength," *Applied Sciences*, vol. 12, no. 23, pp. 1-22, 2022. [CrossRef] [Google Scholar] [Publisher Link]

[39] B.R. Sangeetha et al., "Study of Compressive Strength of Concrete at Elevated Temperature with Different types of Cement and Grades of Concrete," *International Journal of Engineering Technology and Management Sciences*, vol. 7, no. 6, pp. 246-252, 2023. [Google Scholar]

[40] Qingyu Du, and Qi Jiang, "Improvement of Crack Detectivity for Concrete Surface of Subway Tunnels with Anti-Corrosion Coatings using Deep Learning and Image Processing," *Case Studies in Construction Materials*, vol. 22, pp. 1-19, 2025. [CrossRef] [Google Scholar] [Publisher Link]

[41] B. Georgali, and P.E. Tsakiridis, "Microstructure of Fire-Damaged Concrete. A Case Study," *Cement and Concrete Composites*, vol. 27, no. 2, pp. 255-259, 2005. [CrossRef] [Google Scholar] [Publisher Link]

[42] M.M. Morsy, S.S. Shebl, and A.M. Rashad, "Effect of Fire on Microstructure and Mechanical Properties of Blended Cement Pastes Containing Metakaolin and Silica Fume," *Asian Journal of Civil Engineering (Building and Housing)*, vol. 9, no. 2, pp. 95-103, 2008. [Google Scholar]

[43] Hayder Khalid Ali, Sallal R. Abid, and Nildem Tayşi, "Thermal Behaviour and Microstructure of Self-Cured High-Strength Plain and Fibrous Geopolymer Concrete Exposed to Various Fire Scenarios," *Buildings*, vol. 13, no. 10, pp. 1-40, 2023. [CrossRef] [Google Scholar] [Publisher Link]

[44] Kore Sudarshan D, and A.K. Vyas, "Impact of Fire on Mechanical Properties of Concrete Containing Marble Waste," *Journal of King Saud University - Engineering Sciences*, vol. 31, no. 1, pp. 42-51, 2019. [CrossRef] [Google Scholar] [Publisher Link]

[45] Eskinder Desta Shumuye, Jun Zhao, and Zike Wang, "Effect of Fire Exposure on Physico-Mechanical and Microstructural Properties of Concrete Containing High Volume Slag Cement," *Construction and Building Materials*, vol. 213, pp. 447-458, 2019. [CrossRef] [Google Scholar] [Publisher Link]

[46] A.Y.F. Ali et al., "Thermo-Mechanical Behavior and Spalling Resistance of Alkali-Activated Slag Versus Cement Mortars Under Rapid High-Temperature Exposure," *Scientific Reports*, vol. 15, no. 1, pp. 1-29, 2025. [CrossRef] [Google Scholar] [Publisher Link]

[47] Saleh Ahmad Laqsum et al., "Mechanical and Impact Strength Properties of Polymer-Modified Concrete Supported with Machine Learning Method: Microstructure Analysis (SEM) Coupled with EDS," *Journal of Composites Science*, vol. 9, no. 3, pp. 1-26, 2025. [CrossRef] [Google Scholar] [Publisher Link]

[48] Yi Min Wei et al., "A Preliminary Investigation on Microstructural Characteristics of Interfacial Zone Between Cement and Exploded Wood Fiber Strand by using SEM-EDS," *Journal of Wood Science*, vol. 50, no. 4, pp. 327-336, 2004. [CrossRef] [Google Scholar] [Publisher Link]

[49] Bypaneni Krishna Chaitanya et al., "Performance Evaluation of Concrete Containing Fly Ash, Silica Fume and M-Sand Under High Temperatures: Mechanical and Microstructural Approach," *Journal of Infrastructure Preservation and Resilience*, vol. 6, no. 1, pp. 1-17, 2025. [CrossRef] [Google Scholar] [Publisher Link]

[50] Sandra Juradin et al., "Post-Fire Mechanical Properties of Concrete Reinforced with Spanish Broom Fibers," *Journal of Composites Science*, vol. 5, no. 10, pp. 1-17, 2021. [CrossRef] [Google Scholar] [Publisher Link]